

# Atomistic Simulation for Rejuvenation of Cu-Zr Metallic Glasses by Strain

Eunsung Jekal

*Department of materials, ETH Zürich, Zürich, Switzerland*

**Abstract:** Molecular dynamics simulations were carried out to investigate the atomic structure of a model  $\text{Cu}_{64}\text{Zr}_{36}$  bulk metallic glass (BMG). It is found that the amount of icosahedral content of the system is significantly increased in a well relaxed structure. While we considered four connection types of vertex-, edge-, face-, and volume-sharing, the huge cluster in the relaxed samples mainly involve volume-type connection and exhibits a remarkable athermal plasticity that great stiffness and great yield strength compared to the as-quenched samples. In addition, the bond-angle distribution of annealed sample shows sharp peaks at specific bond angles which is an evidence of crystallized Laves-phase formed by icosahedral atoms, however the peaks are to be broaden after loading, which indicates decreasing amount of icosahedral content and their shape distortion. These results suggest that icosahedral content in a bulk metallic glasses plays a key role to determine the mechanical properties such as rigidity and maximum stress carrying capacity.

**Keywords:** Bulk metallic glass; molecular dynamic simulation

## I. INTRODUCTION

### A. Bulk Metallic Glasses

Bulk metallic glasses (BMGs) with a disordered atomic-scale structure exhibit interesting mechanical properties such as extraordinary elastic strain limits and a high tensile yield stress [1–3]. However, their poor ductility is obstructing commercial use of BMGs[4, 5]. To improve it, many efforts are under way, especially in trying to understand the underlying plastic deformation mechanisms in a micro-regime as well as macro-regime. It is generally believed that deformation of amorphous materials such as BMGs depends on emergent processes arising from localized plastic mechanisms. However, how such localized plasticity leads collectively to global failure is still a contemporary topic in the field of BMGs research[6–8].

### B. Current state of BMGs research

Experimentally, structural glasses are produced by the extremely rapid cooling of an under-cooled liquid to avoid formation of long range order and a crystalline phase. As the temperature decreases well below the melting temperatures, a glass transition temperature regime is entered in which atomic motion is exponentially reduced to produce a “frozen” configuration referred to as an amorphous solid. It remains an open question as to how liquid-like this solid structure is. When the initial melt consists of metallic atoms, the resulting amorphous structure is referred to as a BMG. Sizes of the order of a few centimeters can now be created[1–3]. Unlike crystalline solids, plastic deformation mechanisms of amorphous solids are treated by number of local atomic plasticity mechanisms. Spaepen proposed a free-volume model that

single atoms would migrate to a neighboring free-volume region. Later, Argon suggested that several atoms undergo a structural transformation which can modify the local shear stress state [6]. This local plastic process is referred to as a Shear Transformation (ST). In both works of Spaepen and Argon, the proposed local plastic mechanism was assumed to be thermally activated. Such a local mechanism has been observed in several atomistic simulations which studied high-strain rate plasticity in model glass systems [8–11]. These simulation works have inspired the development of the shear transformation zone (STZ) theory. Generally, the STZ theory is considered to be an athermal description of plasticity, where an effective temperature characterizes the structural atomic scale inhomogeneities, which control the STZ activity[12–14]. Experimental results have however suggested thermally activated processes can underly the observed plasticity. For example, Prof. Lofer’s group at ETH Zurich experimentally demonstrated that both propagation and arrest of shear bands are thermally activated processes. Further experimental and theoretical insight into local microscopic plastic processes has been gained within the framework of the under-cooled liquid terminology of  $\alpha$ - and  $\beta$ -relaxation[15–17]. According to the description of relaxation processes in under-cooled liquids introduced by Goldstein,  $\alpha$ -processes (mega-basin in Fig. 1) are considered to be slow and irreversible reorganizations of the undercooled liquid structure which are mediated by the faster and reversible  $\beta$ -processes. In the Potential Energy Landscape (PEL) picture developed by Goldstein for the under-cooled liquid regime, such  $\alpha$  processes represent the traversal from one deep potential energy valley (referred to as a mega-basin) to another, whereas the  $\beta$  process represent the traversal between shallow potential energy valleys that overlay the mega-basin structure. Within this context, the slower  $\alpha$  processes represent the collective effect of many faster  $\beta$  processes. It is however generally believed that as the temperature passes the glass transition regime, the  $\alpha$  processes freeze out to be replaced by a new irreversible mechanism which mediates plasticity at temper-

\* so-young.jekal@mat.ethz.ch

atures well below the glass transition [18].

Over the past few years experimental investigations of BMGs using mechanical spectroscopy methods have become popular. Mechanical spectroscopy is a method which probes relaxation time-scales via the measurement of the frequency dependent storage and loss modulus — probing respectively the elastic and plastic response of the material. Interestingly, such works reveal that either a low temperature tail or a secondary peak in the relaxation modulus exist, both of which have been interpreted as evidence for beta-like relaxation. For example, Fig. 2 shows the temperature  $T$ -dependent loss modulus  $E''$  of the three MG systems.

In Fig. 2, besides the usual  $\alpha$ -relaxation around  $T_g$ , a pronounced  $E''$  peak is observed in the temperature range  $0.60$ - $0.80 T_g$ , corresponding to the  $\beta$ -relaxation in the deep glassy state of Ref. [19], it was hypothesized that the smaller atoms are mainly involved in beta relaxation, whilst collective structural transformations involving the larger atoms were assumed to be necessarily less localized, and those responsible for the primary loss modulus peak (the alpha processes), and therefore macroscopic plasticity. Using the Activation Relaxation Technique nouveau (ARTn) method, Ref. [[20, 21],] investigated the atomic structure of the local structural excitations (LSEs) in model glass with Lennard-Jones (LJ) potential. The ARTn method is a PEL exploration algorithm which identifies transitions between nearby meta-stable structural states, and has been used in the past to investigate structural transitions in glasses. Inspection of the atomic displacement vector between the two considered meta-stable states, reveals the corresponding structural transformation to be localized, involving only a few atoms, and hence the terminology of the LSE. This work found that the smaller and more weakly bonded atoms are dominantly involved in LSEs, which often occurred near regions of excess free volume. Furthermore, the LSEs (in terms of atomic displacement) were string-like mainly involving less than six atoms, each with a displacement generally comparable to the bond length shown in Fig. 3.

Such string-like local structural excitations have also been observed in the under-cooled liquid regime as the temperature approaches (from above) the glass transition regime, and have been associated with the emerging slower structural relaxation processes of growing structural dynamical heterogeneities. The consequence of such dynamics on structure close to (and below) the glass transition regime remains an active topic of research — posing the question of how different the amorphous structure is to that of a liquid. In fact from a static perspective, the structure of a glass forming liquid does not show any strong structural change as the system passes through the glass transition. Clearly new length and time-scale correlations grow and some form of medium range order emerges. The project is interested in similar questions, but rather from the amorphous solid perspective, that is, at temperatures well below the glass

transition regime.

For example, how does collective LSE activity affect structure and underly plasticity? In the 1980s, Nelson and co-workers considered the amorphous solid in terms of local icosahedral structure, demonstrating that the transition to a glass (from an under-cooled liquid) is characterized by an increasing number of local atomic environments with an approximate icosahedral symmetry. This is driven by the desire of the system to optimally minimize bond energy and therefore bond frustration. Indeed the work of Nelson demonstrated the rigidity of the amorphous material may be related to the topological nature of how such structures are connected with each other. These ideas naturally led to topic of the connectivity of local icosahedrally coordinated environments. Since then some work has been done in attempting to understand both structure and deformation in terms of such local order (short-range) and its connecting (medium range). Recently, Ma and co-workers published a paper which includes a detailed analysis of atomic packing of ab initio molecular dynamics data binary systems. They found that for binary BMGs, where the solute species is in a minority, a wide range of local Kasper polyhedra as well as icosahedra describe the local environment of the solute atom. This work also found that the packing behaviours of such polyhedra which can give geometrical insight into the medium range order of BMGs. Such phenomena with respect to temperature, time, and athermal plastic evolution, can be studied using atomistic simulation methods. In fact, a direct correlation between quenching rate and icosahedral content, where the slower quench makes the larger the fraction of icosahedral order within the sample. The general finding is that the higher the icosahedral content is in an amorphous sample, the more relaxed the sample is. Furthermore, simulations confirmed that maximal icosahedral content leads to maximal plastic localization and the athermal formation of shear bands. Moreover, in the atomic scale regions where the shear banding occurs, the icosahedral content reduces. In this regime of plastic activity, the full-icosahedral content is partially destroyed with the geometric structures becoming fragmented. Such a picture was recently used to discuss deformation experiments performed in Prof. Lofer group in ETH Zurich investigating shear band velocities.

The present work's central goal is to investigate how such LSE structural excitations collectively affect structure. In particular, how do they modify icosahedral content and possibly induce medium range order from the perspective of icosahedral structure packing? How is such short and long range correlations affected by high-strain rate plasticity will also constitute a large part of this work. To do this, a more realistic metallic force model, representing the binary Cu-Zr BMG system, will be investigated as a function of atomic fraction.

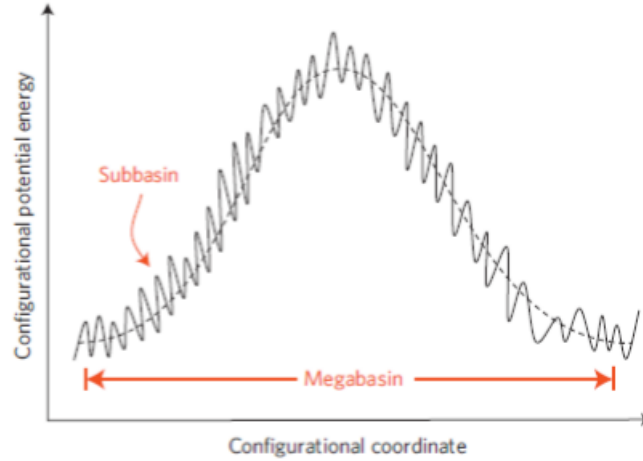


FIG. 1. Schematic of the potential energy landscape for a metallic glass.[26]

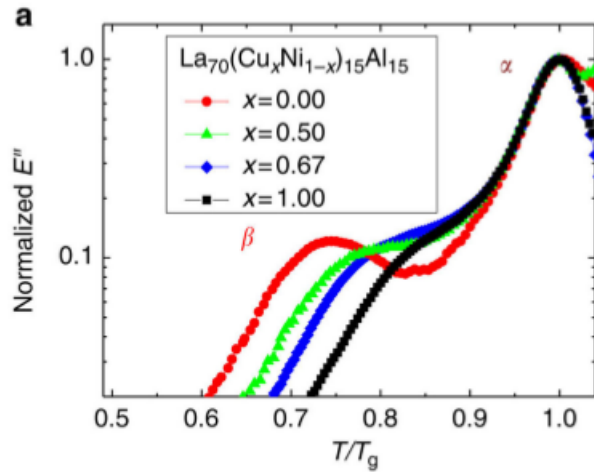


FIG. 2. Six examples of LSEs. In each case, the initial atomic positions are visualized by green balls and the final ones by orange balls. The atomic displacements from the initial to activated and activated to final states are visualized by red and blue arrows, respectively.

## II. METHODS

### A. Atomistic simulation methods

Molecular dynamics (MD) simulation[22] and activation-relaxation technique (ART) method would be mainly used in this study. Even though glass samples are produced by MD, only a few seconds of simulation time are routinely accessible. To overcome time scale problem, ART method is applied to investigate atomic activity in perspective of potential energy landscape (PEL). As shown in Fig. 2 which represents PEL, ART is used to explore the potential energy landscape around a local

minimum energy configuration, and the properties of local minimums and their surroundings are investigated by MD.

**Molecular Dynamics** To investigate local structures and mechanical properties of Cu-Zr binary alloys, the molecular dynamic simulation has been carried out using the Large-scale Atomic/Molecular Massively Parallel Simulator (LAMMPS) package [64]. For empirical potential the embedded-atom (EAM) potential developed by Mendelev et al. is adapted. In an EAM potential, the potential energy of a particular atom,  $i$ , is given as

$$V_i = F_\alpha \left[ \sum_{i \neq j} \lambda_\beta(r_{ij}) \right] + 12 \sum_{i \neq j} \Phi_{\alpha\beta}(r_{ij}) \quad (1)$$

where  $F_\alpha$  is an embedding function which represents the energy required to place atom  $i$  in the host electron cloud of the metal,  $\rho_\beta$  is the electron density at the site  $i$  due to the surrounding atoms. Here,  $\alpha$  and  $\beta$  correspond to the species type of atoms  $i$  and  $j$ , respectively.  $\Phi_{\alpha\beta}$  is a pairwise potential function, and lastly  $r_{ij}$  is the distance between atoms  $i$  and  $j$ . Compare to LJ potential which considers only the distance between the particles, EAM potential is particularly appropriate for metallic systems.

### B. Activation-Relaxation Technique (ART)

To obtain a large number of LSEs and to compare it with results from MD, the ART method is applied to Cu-Zr binary BMGs. Using these data, a statistical analysis will be performed. The ART is a search method for finding local transition states via an analysis of the PEL curvature. ART proceeds in three steps. First, starting from a meta-stable state, the configuration is deformed in order to identify a direction of negative curvature on the energy landscape. Then, it converges to a first-order saddle

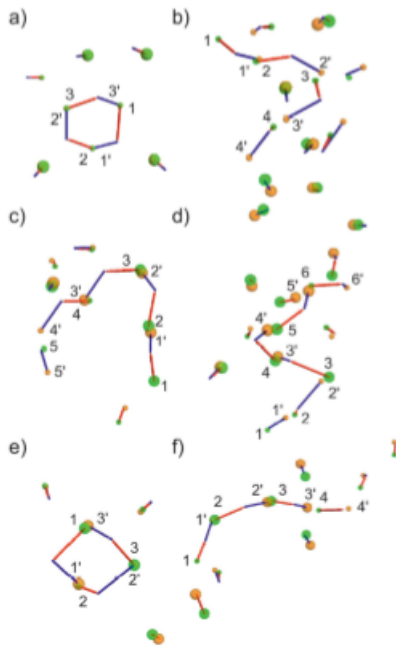


FIG. 3. Schematic diagram of ARTs and MD methods.

point. Once a direction of negative curvature is identified, the system is pushed along this direction. Finally they are relaxed into a new minimum. To find the new minimum, it pushes the configuration over the transition state and relax the total energy. These steps form an event, a set of three related configurations: the initial minimum, the transition state, and the final minimum. The event can be used to characterize the local energy landscape. However, there are currently limitations since it can not measure beta-relaxation processes which have a important correlation with properties of BMGs, such as aging, diffusion and plastic deformation.

### C. Preliminary results

The preliminary results represent a part of the familiarization phase of the project. In particular, focused knowledge and experience of the LAMMPS package and the ARTn modification is gained for the creation and relaxation of a model binary Cu-Zr glass systems.

### D. preparation + analysis of atomic structure/activity

Here, the sample preparation procedure developed in ref.[40] for the Lennard Jones model potential is applied to the CuZr EAM potential system. This will be done for a variety of stoichiometric combinations.

### 1. Quench/Anneal protocol

Amorphous  $\text{Cu}_{50}\text{Zr}_{50}$ ,  $\text{Cu}_{64}\text{Zr}_{36}$ , and  $\text{Cu}_{75}\text{Zr}_{25}$  samples, with a total number of 3000 and 24'000 atoms, were prepared. Starting from a cubic crystallized arrangement with a random chemical arrangement, samples were melted at 4000 K and equilibrated during 10 ns using an NVT ensemble (xed volume conditions). Temperature control was done via a Nose-Hoover method. Then, using an NPT ensemble (xed pressure conditions) they were quenched to a temperature of 50 K, using a cooling rate of  $1.95 \times 10^{10}$  K/s. We refer to these samples as "as-quenched". Such quenches were also interrupted, and held at chosen xed temperatures for chosen time periods, after which the quench was continued down to a temperature of 50 K. These samples are referred to as "annealed" samples. The chosen temperatures (in terms of the glass transition temperature  $T_g$  — to be dened) are  $0.9 T_g$ ,  $0.5 T_g$ , and  $0.1 T_g$  and the time period is 600 ns. Fig. 5(a) displays system volume per atom as a function of temperature for the uninterrupted quench, for three different chemical compositions. Such a protocol produces the as-quenched samples. Inspection of this figure reveals a change in slope of two approximately linear regimes and indicates a transition from a liquid-like to a glass-like structure. The intersection of these two lines is dened as the ctive glass transition temperature and throughout this work will be referred to as the glass transition temperature  $T_g$ . There is volume contraction. Gray lines represent a linear fitting to clarify a ctive glass transition temperature. As shown in Fig. 5(a) the ctive  $T_g$  monotonically decreases from 1030 K to 910 K with an increase in the Cu concentration. This trend is also seen in experiment. Fig. 5(b) plots the corresponding percentage of icosahedrally coordinated atoms as a function of temperature. The icosahedral content is determined via a Voronoi tessellation of the atomic positions, each atom constituting a Voronoi center. The atoms whose Voronoi volume has twelve faces are dened as being icosahedrally coordinated. The atomic visualization software, OVITO[23], is used to do this. The figure shows that the liquid state contains only a few icosahedra, however as the temperature reduces and the glass transition regime is entered, the icosahedral content rapidly increases. Below the glass transition it then more gradually increases. Data is also included from the annealing protocol, in which the sample was held at  $0.9 T_g$  for 600 ns followed by a direct quench to 50 K. The figure show that annealing the sample close to the  $T_g$  results in a significant increase in icosahedral content. These samples are therefore significantly more relaxed. Fig. 5(c) plots the atomic positions of the icosahedrally coordinated atoms of one particular sample. The atoms are colored according to the cluster of icosahedrally atoms it is (nearest neighbour) connected to, where red represents the largest cluster and blue the smallest cluster. The left and right panels show configurations for a content of respectively 10% and 33% — the latter being the more relaxed configuration. What



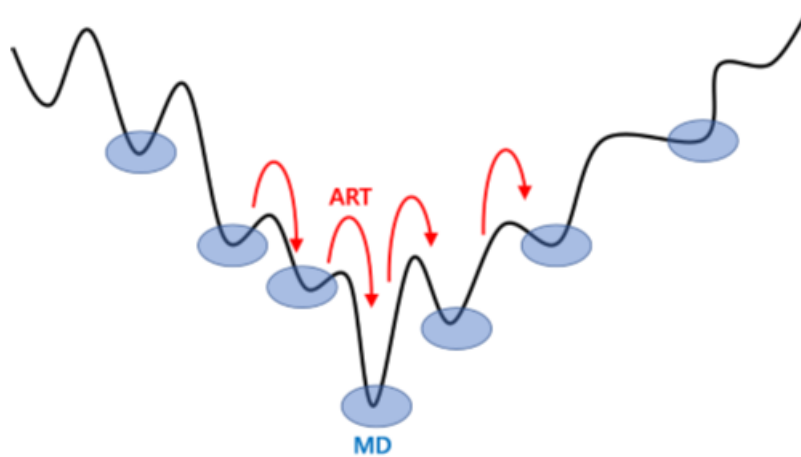


FIG. 4. (a) Temperature dependencies of system volume with different amount of Cu. Gray solid lines represent a linear fitting to clarify a fictive glass transition temperature. (b) Percentage of icosahedra as a function of temperature. Dotted and solid lines represent as-quenched and 600 ns annealed samples, respectively. (c) Illustrative simulation snapshots depicting the icosahedra networks. While coloring indicates a size of cluster, blue and red color correspond with the smallest and the biggest clusters, respectively. (d) Percolation of icosahedra network. Black and blue lines correspond samples with 3000 and 24000 atoms, respectively.

becomes apparent, is the growth of a single icosahedral cluster that percolates the entire simulation cell. Fig. 5(d) plots the largest cluster of a configuration as a function of that configuration's icosahedral content. Here the configurations are taken from the quench protocol used to produce the final sample. Thus, via Fig. 5(b), the icosahedral content represents a temperature. Two different sample sizes are shown. It demonstrates that during the quench protocol, as the temperature reduces and enters the glass transition regime, a single large connected cluster of icosahedral atoms rapidly emerges to percolate the system. Fig. 5(d) indicates a sharpening of the transition and might suggest a percolation transition — this aspect will be investigated in more detail in future work. Such a percolating structure, which is known to be more relaxed than the remainder of the material can have important consequences for the rigidity and also material strength.

## 2. LSEs observed from MD

Here thermally activated atomic displacements, corresponding to structural transformations occurring at finite  $T$  during sample preparation are investigated. Such displacements are studied by investigating the atomic motion between two configurations which have been relaxed to their local minimum via a conjugate gradient method. Any observed displacement represents the structural change needed to go from one local minimum to another. Fig. 6 presents LSEs arising from a  $\text{Cu}_{64}\text{Zr}_{36}$  configuration which are formed at different annealing temperatures of (a)  $T_g$ , (b)  $0.9T_g$ , (c)  $0.5T_g$ , and (d)  $0.1T_g$ . In Figs. 6(a-c), there are several local displacements in the form of sequential string-like motion in which the position

of one atom is replaced by another neighbouring atom. structures. Whilst both Cu and Zr can be involved in the LSE activity, Cu is more often seen to participate in this string-like activity. This trend is also observed in samples containing more Cu, where in the  $\text{Cu}_{75}\text{Zr}_{25}$  sample the LSEs are completely dominated by the Cu. Only short atomic displacements less than  $0.5 \text{ \AA}$  are found in Fig. 6(d). These results are similar to what was seen for a Lennard Jones model binary glass, where at low temperatures the LSE are found to be less local and consisting of sub-bond length displacements.

## 3. LSEs observed from ARTn

The ARTn algorithm has been applied repeatedly to the zero temperature samples, each time starting with a randomly chosen initial atomic displacement, resulting in many converged saddle-point configurations and new nearby local PEL minima. In this context, an LSE is defined as the structural process which leads to the system being (thermally) excited to the saddle-point and finally to the local PEL minimum. The corresponding LSE barrier energy is the difference in energy between the initial configuration and the saddle-point configuration. Fig. 7(a) plots histograms of the barrier energies found by ARTn for the three considered chemical compositions. The distributions are similar to that seen in the model Lennard Jones systems, and characterized by a central peak and a low barrier energy tail. Fig. 7(a) shows that the sample with higher Cu concentration has tends to have a distribution that is shifted to lower barrier energies suggesting atoms with the smaller volume can move more easily — a result which is compatible with the previous section on

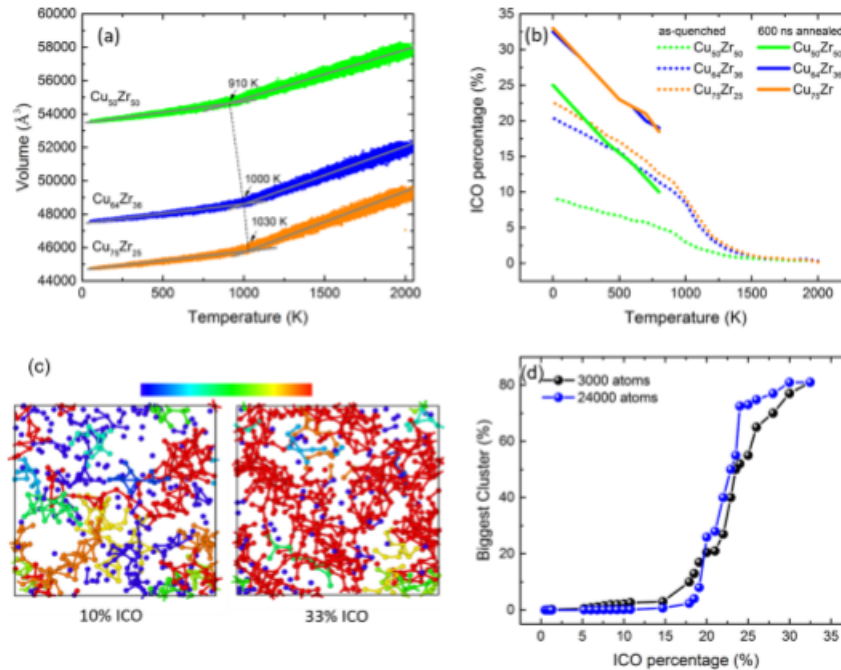


FIG. 5. Atomic displacement map at (a) the  $T_g$ , (b)  $\sim 0.9T_g$ , (c)  $\sim 0.5T_g$ , and (d)  $\sim 0.1T_g$ . Red and blue balls correspond to the Cu and Zr atoms, respectively. Each vector indicates the atomic displacement from the initial position to final position during 1 ps. Only atoms whose displacement is greater than 1.3  $\text{\AA}$  and 0.5  $\text{\AA}$  are shown in (a-c) and (d), respectively. Figures are visualized via OVITO with 24000 number of atoms.

MD work and also accords with ref.[24]. Fig. 7(b) shows an LSE of  $\text{Cu}_{50}\text{Zr}_{50}$  with a barrier energy of 5.2 eV. Although smaller atoms are more involved in the formation of the string, two Zr atoms contribute are involved in this structural excitation. Fig. 7(c) represents an LSE of  $\text{Cu}_{64}\text{Zr}_{36}$  with a barrier energy of 4.0 eV and also shows a string-like atomic reconfiguration with now only one Zr atom. Finally, an LSE of  $\text{Cu}_{75}\text{Zr}_{25}$  with a relatively low barrier energy of 3.85 eV is depicted in Fig. 7(d) now containing only Cu atoms. Thus, for this more realistic CuZr alloy systems, both the ARTn and direct MD at finite temperature display similar LSE structures and trends.

#### 4. Connectivity of icosahedra

In Fig. 5, we observed the percentage of icosahedrally coordinated atoms greatly increases when the system is annealing process at  $0.9T_g$  for 600 ns. In this present section, we demonstrate preliminary work investigating the nearest neighbour connectivity of the developing icosahedral structure using a classification scheme proposed in Ref. [25]. In Ref. [25] icosahedrally coordinated atoms are classed as vertex (sharing one common nearest neighbour atom), edge (sharing two atoms), face (sharing three atoms) and volume (sharing four atoms)—see the upper

panel of Fig. 8 taken directly from Ref.[25]. Here, we investigate the creation of these icosahedra connections with respect to the annealing time to understand in more detail how the icosahedral structure percolates through the system. Fig. 8 quantifies the connections between icosahedra as a function of time, as the Cu-Zr alloys are annealed at 800 K. Plotted, is the percentage breakdown of connectivity types of the increasing population of icosahedrally coordinated atoms. Note that the absolute percentage of icosahedrally coordinated atoms is in the range of 10% for the  $\text{Cu}_{50}\text{Zr}_{50}$  sample and up to 20% for the samples with higher Cu content. Fig. 8 shows that for the  $\text{Cu}_{64}\text{Zr}_{36}$  and  $\text{Cu}_{75}\text{Zr}_{25}$  samples, there are no disconnected icosahedral atoms, whereas in the  $\text{Cu}_{50}\text{Zr}_{50}$  sample there is constant population. Since icosahedral content scales with Cu content, this result demonstrates that when the Cu content is low enough there will always exist isolated icosahedral environments. As structural relaxation proceeds volume connectivity eventually dominates in the  $\text{Cu}_{64}\text{Zr}_{36}$  and  $\text{Cu}_{75}\text{Zr}_{25}$  samples. This is plausible because of the higher absolute density of icosahedral content in these samples. For the  $\text{Cu}_{50}\text{Zr}_{50}$  sample face connectivity remains slightly dominant over volume connectivity, a result that is compatible with the lower absolute icosahedral content of this Cu composition. It is emphasized that these results are valid only for the sub-microsecond relaxation time-scale.

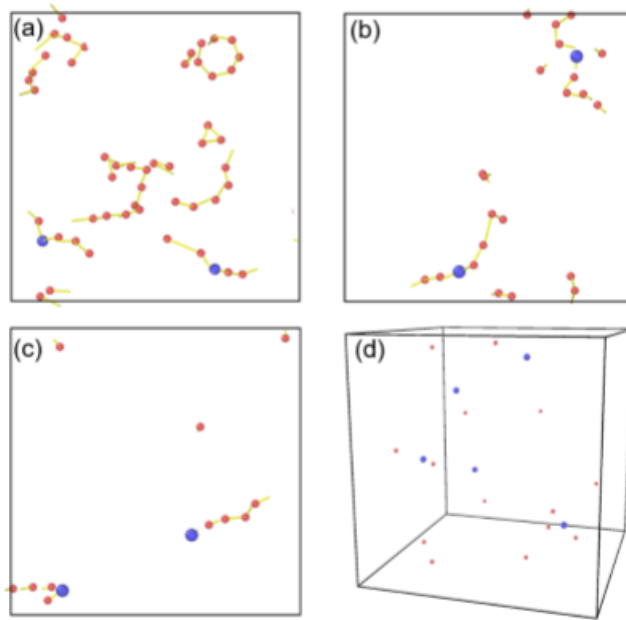


FIG. 6. (a) Histogram of participation number. (b) LSEs of  $\text{Cu}_{64}\text{Zr}_{36}$ .

### E. Mechanical properties

Because of the short time-scale restriction of the MD method, nite temperature atomistic simulations of deformation can mainly probe the highstrain rate athermal limit of plasticity. In this section we investigate the effect different chemical composition and degree of relaxation has on athermal plasticity, and study how such plasticity affects the underlying icosahedral structure. To do this, the three samples of  $\text{Cu}_{50}\text{Zr}_{50}$ ,  $\text{Cu}_{64}\text{Zr}_{36}$ , and  $\text{Cu}_{75}\text{Zr}_{25}$  were subjected to uniaxial tensile loading at a constant strain rate on the order of  $10^9\text{s}^{-1}$  at a temperature of  $T_g$ . The resulting stress-versus-strain graphs for the three samples are plotted in Fig. 9(a) and reveal an initial elastic response, followed by a peak stress response at elevated stresses, and nally a ow stress response at reduced stresses. Inspection of this gure demonstrates the peak yield stress and subsequent ow stress increase with increased Cu concentration. The results are in agreement with previously reported simulation work. Fig. 9(b) shows the stress-strain curves for the as-cast and annealed samples. The annealed samples show a greater initial peak stress (which increases with annealing simulation time) than that of the as-cast sample. At large enough strains the subsequent ow stress is found to be independent of the degree of relaxation.

As the plastic strain evolves beyond the peak stress response, the icosahedral content drops in all samples indicating structural excitation — rejuvenation. Using the nearest neighbour connectivity classication scheme this break up of the icosahedral structure can now be better

understood. Fig. 10 plots the percentage breakdown of the icosahedral connectivity as a function of strain for the three considered compositions. Inspection of this data reveals a change in all types of connectivity as the absolute population of icosahedral content reduces (not shown). The percentage of isolated icosahedral environments increases, as does the vertex and edge connectivity types. On the other hand the face and volume connectivity types decrease for all chemical concentrations. Interestingly, the volume connectivity which is the only type to show an increase with annealing reveals the most rapid decline. Together this suggests that as athermal plasticity proceeds and the structural state is excited (rejuvenated) the initial percolated icosahedral cluster undergoes fragmentation. This process occurs mainly in the transition regime from elasticity to plasticity, when the system's stress is at its maximum. Together, these results imply a central role for icosahedral content in an amorphous structure (as alluded to in past works [58]), in relation to its rigidity and maximum stress carrying capacity. The present preliminary work goes one step further in quantifying how the icosahedral backbone is broken up in the limit of anthermal plasticity, and will form the basis of the rst manuscript of the project intended for submission to a referred journal.

### III. OPEN QUESTION AND PLAN

From the current state of research and the preliminary work this project will address a number of open questions and issues. These are

1. Both MD and the ARTn method reveal localized structural excitations taking the form of extended string-like atomic displacements. The structural environment around such LSEs has yet to be investigated in terms of icosahedral content and connectivity. This will be done in the present project. In particular, does the extended string-like geometry of the LSE correlate with the surrounding icosahedral structure? Is there a statistical difference in the energy landscape for LSEs associated with the creation of icosahedral structures?

2. How does collective LSE activity lead to the medium range order associated with icosahedral connectivity? This focus will try to gain a microscopic understanding of how emergent processes occur leading to significant structural relaxation and plasticity. It is envisioned that such work will give a better understanding of the analogy to the under-cooled liquid terminology of alpha and beta processes.

3. How does the icosahedral structure lead to a rigid structure? Where does the rigidity break down and why? This questions will be addressed via high-strain rate athermal MD simulations, and essentially involve investigation of the athermal yielding process. Once in the

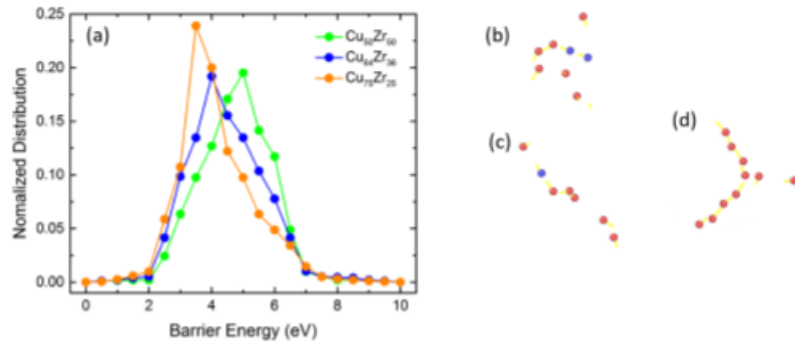


FIG. 7. (a) Histogram of participation number. (b) LSEs of  $\text{Cu}_{64}\text{Zr}_{36}$ .

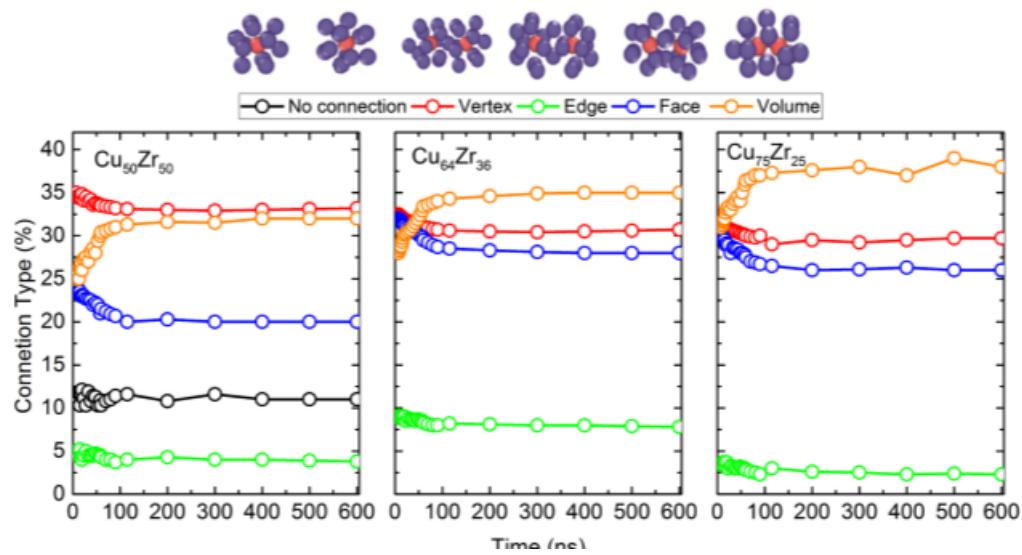


FIG. 8. The percent of connection types between icosahedra in  $\text{Cu}_{50}\text{Zr}_{50}$ ,  $\text{Cu}_{64}\text{Zr}_{36}$ , and  $\text{Cu}_{75}\text{Zr}_{25}$ . The different types of connections between icosahedra is depicted on top.

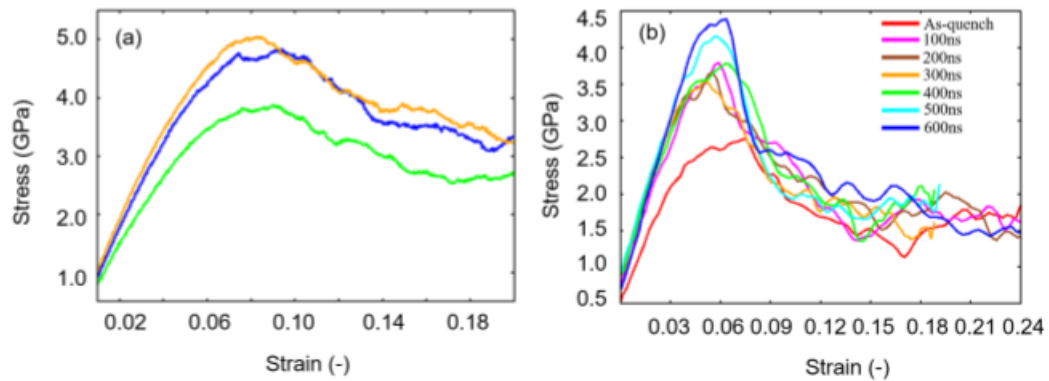


FIG. 9. Uniaxial tensile loading stress versus strain for  $\text{Cu}_{50}\text{Zr}_{50}$ ,  $\text{Cu}_{64}\text{Zr}_{36}$ , and  $\text{Cu}_{75}\text{Zr}_{25}$  at constant strain rate of 109 s<sup>-1</sup>.



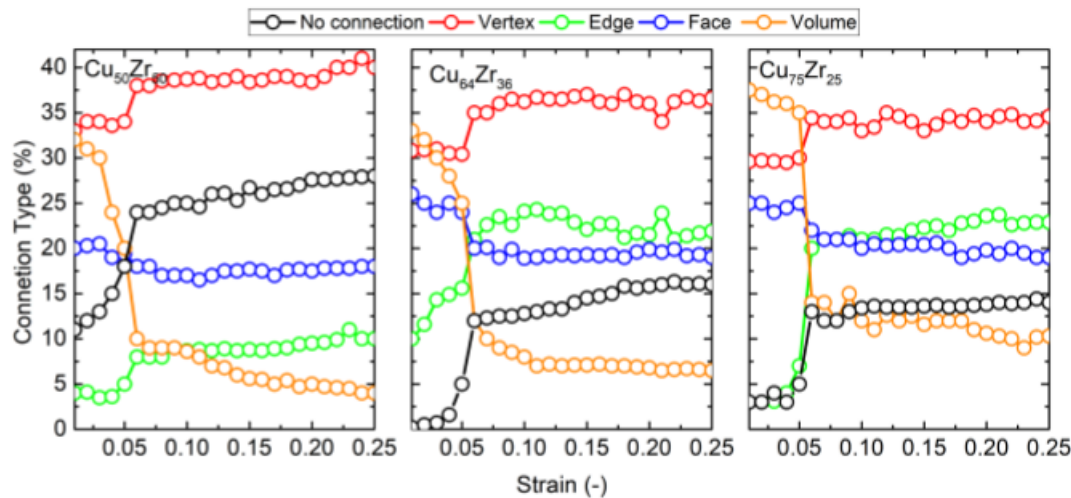


FIG. 10. The percent of connection types between icosahedra in  $\text{Cu}_{50}\text{Zr}_{50}$ ,  $\text{Cu}_{64}\text{Zr}_{36}$ , and  $\text{Cu}_{75}\text{Zr}_{25}$  as a function of strain.

plastic ow regime (after yield), how does the icosahrdal structure evolve? In particular what aspects of its (broken) connectivity dominate the rejuvenation of the structure? Although the athermal plastic limit is far from experiment, such work can give upper limits to how much energy can be stored (and how) in an amorphous structure via mechanical work. Points 1 and 2 will exploit both direct MD at nite temperature and the PEL exploration method of ARTn, whereas point 3 will rely on direct MD to probe athermal plasticity. In the rst instance, the approach taken will be related to earlier works, which

investigated how such icosahedra may evolve depending on atomic composition, temperature, and annealing time. Analysis of icosahedral structure with respect to relaxation and plasticity will rstly employ the past work of Ref. [25], using the nearest neighbour connection types of vertex-, edge-, face-, and volume-sharing. As done in the case of Figs. 0.8 and 0.10. It is however anticipated that a new analysis method will be developed with respect to the “disclination” bond defect originally introduced by David Nelson. Such an approach will allow for more distant connectivity to be investigated and classied.

- [1] D. V. Louzguine, A. R. Yavari, and A. Inoue, Devitrification behaviour of cu-zr-ti-pd bulk glassy alloys, *Philosophical Magazine* **83**, 2989 (2003).
- [2] A. Inoue, B. Shen, H. Koshiha, H. Kato, and A. R. Yavari, Cobalt-based bulk glassy alloy with ultrahigh strength and soft magnetic properties, *Nature materials* **2**, 661 (2003).
- [3] X. Gu, A. McDermott, S. J. Poon, and G. J. Shiflet, Critical poisson’s ratio for plasticity in fe-mo-c-b-ln bulk amorphous steel, *Applied Physics Letters* **88**, 211905 (2006).
- [4] H. Bruck, T. Christman, A. Rosakis, and W. Johnson, Quasi-static constitutive behavior of zr41. 25ti13. 75ni10cu12. 5be22. 5 bulk amorphous alloys, *Scripta Metallurgica et Materialia* **30**, 429 (1994).
- [5] C. Barrett and T. Massalski, *Structure of metals 3rd revised edition: Crystallographic methods, principles, and data*, international series on materials science and technology, 35 (1987).
- [6] S. Jekal, P. Derlet, and J. Löffler, Geometrical characterization of atomic structure of cu-zr bulk metallic glasses, (2018).
- [7] F. Albano and M. L. Falk, Shear softening and structure in a simulated three-dimensional binary glass, *The Journal of chemical physics* **122**, 154508 (2005).
- [8] K.-W. Park, C.-M. Lee, M. Wakeda, Y. Shibutani, M. L. Falk, and J.-C. Lee, Elastostatically induced structural disordering in amorphous alloys, *Acta Materialia* **56**, 5440 (2008).
- [9] K.-W. Park, J.-i. Jang, M. Wakeda, Y. Shibutani, and J.-C. Lee, Atomic packing density and its influence on the properties of cu-zr amorphous alloys, *Scripta Materialia* **57**, 805 (2007).
- [10] S. M. Foiles, M. Baskes, and M. S. Daw, Embedded-atom-method functions for the fcc metals Cu, Ag, Au, Ni, Pd, Pt, and their alloys, *Physical review B* **33**, 7983 (1986).
- [11] M. W. Finnis and J. E. Sinclair, A simple empirical n-body potential for transition metals, *Philosophical Magazine A* **50**, 45 (1984).
- [12] D. J. Evans and B. L. Holian, The nose-hoover thermostat, *The Journal of chemical physics* **83**, 4069 (1985).
- [13] D. Xu, B. Lohwongwatana, G. Duan, W. L. Johnson, and C. Garland, Bulk metallic glass formation in binary cu-rich alloy series-cu100- xzrx (x= 34, 36, 38.2, 40 at.%) and mechanical properties of bulk cu64zr36 glass, *Acta Materialia* **52**, 2621 (2004).
- [14] W. L. Johnson, Bulk glass-forming metallic alloys: Science and technology, *MRS bulletin* **24**, 42 (1999).

- [15] C. A. Schuh, T. C. Hufnagel, and U. Ramamurty, Mechanical behavior of amorphous alloys, *Acta Materialia* **55**, 4067 (2007).
- [16] M. F. Ashby and A. L. Greer, Metallic glasses as structural materials, *Scripta Materialia* **54**, 321 (2006).
- [17] W.-H. Wang, C. Dong, and C. H. Shek, Bulk metallic glasses, *Materials Science and Engineering: R: Reports* **44**, 45 (2004).
- [18] C. Maloney and A. Lemaitre, Subextensive scaling in the athermal, quasistatic limit of amorphous matter in plastic shear flow, *Physical review letters* **93**, 016001 (2004).
- [19] A. Inoue, Stabilization of metallic supercooled liquid and bulk amorphous alloys, *Acta materialia* **48**, 279 (2000).
- [20] S. Swayamjyoti, J. F. Löffler, and P. Derlet, Local structural excitations in model glasses, *Physical Review B* **89**, 224201 (2014).
- [21] S. Swayamjyoti, J. F. Löffler, and P. Derlet, Local structural excitations in model glass systems under applied load, *Physical Review B* **93**, 144202 (2016).
- [22] S. Plimpton, P. Crozier, and A. Thompson, Lammmps-large-scale atomic/molecular massively parallel simulator, *Sandia National Laboratories* **18** (2007).
- [23] A. Stukowski, Visualization and analysis of atomistic simulation data with OVITO—the open visualization tool, *Modelling and Simulation in Materials Science and Engineering* **18**, 015012 (2009).
- [24] A. J. Cao, Y. Q. Cheng, and E. Ma, Structural processes that initiate shear localization in metallic glass, *Acta Materialia* **57**, 5146 (2009).
- [25] M. Lee, C.-M. Lee, K.-R. Lee, E. Ma, and J.-C. Lee, Networked interpenetrating connections of icosahedra: Effects on shear transformations in metallic glass, *Acta Materialia* **59**, 159 (2011).